Fractal Analysis of Noise Signals of Sampo and John Deere Combine Harvesters in Operational Conditions

Farzad Mahdiyeh BOROUJENI[(1)], Ali MALEKI[(2)*]

[(1)] *Mechanical Engineering of Biosystems*
Shahrekord University
Iran; e-mail: 1404.farzad@gmail.com

[(2)] *Department of Mechanical Engineering of Biosystems*
Shahrekord University
Shahrekord, Iran
[*]Corresponding Author e-mail: maleki@sku.ac.ir

Combine harvesters are the source a large amount of noise in agriculture. Depending on different working conditions, the noise of such machines can have a significant effect on the hearing condition of drivers. Therefore, it is highly important to study the noise signals caused by these machines and find solutions for reducing the produced noise. The present study was carried out is order to obtain the fractal dimension (FD) of the noise signals in Sampo and John Deere combine harvesters in different operational conditions. The noise signals of the combines were recorded with different engine speeds, operational conditions, gear states, and locations. Four methods of direct estimations of the FD of the waveform in the time domain with three sliding windows with lengths of 50, 100, and 200 ms were employed. The results showed that the Fractal Dimension/Sound Pressure Level [dB] in John Deere and Sampo combines varied in the ranges of 1.44/96.8 to 1.57/103.2 and 1.23/92.3 to 1.51/104.1, respectively. The cabins of Sampo and John Deere combines reduced and enhanced these amounts, respectively. With an increase in the length of the sliding windows and the engine speed of the combines, the amount of FD increased. In other words, the size of the suitable window depends on the extraction method of calculating the FD. The results also showed that the type of the gearbox used in the combines could have a tangible effect on the trend of changes in the FD.

Keywords: sound; combine; fractal dimension; engine speed; sliding window.

1. Introduction

Agriculture workers (farmers) are faced with an extensive range of harmful elements. Physical hazards caused by agricultural machineries and animals may lead to injuries. At the same time, most agricultural jobs are accompanied with noise, which affects the hearing ability (McBride *et al.*, 2003). Agriculture is one of the three top jobs known for dealing with high amounts of noise. However, it is not common to use hearing protection devices among farmers. It is still unknown at what age hearing decrease related to noise in agriculture starts; however, it is quite common among those who work on farms (Ehlers, Graydon, 2011). Nowadays, the source, type, and effects of noise

in relation to its spread time in agricultural machinery have been taken into account in numerous studies. Such studies need to be continued until it is determined what type of absorbing material and at what sound pressure levels lead to a decrease in the scale of hearing-basis noise (Aybek *et al.*, 2010). Therefore, analysing noise signals is an influential step in determining the elements that cause and intensify noise.

Fractals provide us with a new method of characterising seemingly complex and irregular structures in nature by means of the fractal dimension. The term "fractal dimension" (FD) refers to a non-integer or fractional dimension of a geometric object. Application of FD includes two views: one in time domain and the other in phase space domain. The first view pre-

supposes estimating FD directly in the time domain or original waveform domain, where the waveform or original signal is considered a geometric figure (ESTELLER *et al.*, 2001). It has been used extensively in modelling of self-similar structures such as mountains, clouds, rocks, etc. Self-affinity can be found in thermal noise, human electroencephalogram (EEG), music, and recently in vocal sounds (SABANAL, NAKAGAWA, 1996).

Every noise signal in time domain is like a flat curve, and the fractal geometry is a tool to study this type of waveform. According to the geometric structure, fractal refers to the objects which are similar in different scales of length (RANGAYYAN *et al.*, 2013).

FD indicates important features of a signal and includes data on its structural complexity. Known signals like noise signals, fractal Brownian motion, physiologic signals, and so on, have fractal features. It is noteworthy that every flat curve (waveform) with Hausdorff dimension between 1 and 2 is a fractal form. In fractal geometry, FD is a statistical quantity that determines how the space is filled with a phenomenon; therefore, there are various special methods for its determination (RAGHAVENDRA, NARAYANA DUTT, 2010).

Three waveform FD analyses of flow-specific lung sounds had been compared to examine the fractal nature of these signals. FDs of time-domain lung sounds were calculated within three running windows of lengths 200, 100, and 50 ms. The results showed all FDs increased, though the FD method incorporating morphological normalisation exhibited the least increase (GNITECKI, MOUSSAVI, 2005). GOMEZ *et al.* (2009) employed Higuchi's method to calculate the FD of MEG signals in Alzheimer's patients. The results indicated that FD of the patients' signal was lower than that of the control ones. In other words, there was an unusual dynamic state among the Alzheimer's patients.

KLONOWSKI *et al.* (2005) indicated that each state of sleep can be described using a certain range of the Higuchi's FD. They observed that the FD of brain signals during awake times was at maximum among for healthy individuals and those with insomnia, and it dropped during deeper sleep. BOHEZ and SENEVIRATHNE (2001) used FD to distinguish phoneme (sound) and segmentation of words. XIE *et al.* (2011) utilised the geometric analysis in 3D distribution of the output sound during stone damage and breakage process. Increased FD is appropriate to low stress and high released energy, which is in accord with theoretical analyses. The FD obtained from examinations of non-axial stress and indirect tension is respectively below 2.20 and 2.57.

BRUNO *et al.* (2008) discuss methods of identifying plants by analysing leaf complexity based on estimating their FD. Leaves were analysed according to the complexity of their internal and external shapes. The results showed the best approach to analyse shape

complexity based on FD. A high-throughput method allowing the measurement of maize root traits was expressed in a FD calculated from root images. FD values were obtained from different views of a root system. All correlation coefficients determined using marginal means of FDs were highly significant ($P < 0.001$) and ranged from 0.77 to 0.83 between FD values obtained from lateral and top images combined, and from 0.83 to 0.88 for FD values determined for lateral images only (GRIFT *et al.*, 2011).

By means of theoretical analysis of the relationship between the FD of blasting fragments and the dynamite specific energy, a mechanical model for describing the size distribution of top-coal and the dissipation of blasting energy was proposed by XIE and ZHOU (2008). The results showed that the FD of coal fragments could be used as an index for optimising the blasting parameters for a top-coal weakening technique. BACKES and BRUNO (2010) introduced a novel approach for shape classification using complex network and multiscale fractal dimension. Their results reported a powerful potential of discriminating classes, overcoming the results of traditional shape analysis methods, such as curvature, Fourier descriptors, Zernike moments, Bouligand-Minkowski, and Skeleton Paths.

The examples of fractal dimension applications are in a wide range and can be found in areas as distinct as medicine, texture analysis, geology, botany, materials engineering, electronics, physics, histology, soil analysis, plant diseases, polymer analysis (FLORINDO, BRUNO, 2011), electroencephalogram (EEG) and electrocardiogram (ECG) signals, etc. There also exists some research on FD of off-road vehicle sound signals, in particular, agricultural combine harvesters. In this study, FDs have been calculated for noise signals of two combine harvesters in different type of operations, engine speeds, gear ratios with different sized windows. Katz, Sevcik, Higuchi, and MRBC methods were employed for calculation of noise signals FD. It is hypothesised that using signal FD can be a promising way to find a new method in acoustic complexity analysis, and if combine's noise signals are self-similar, FD values should not change substantially with window size or signal amplitude scaling within particular events of the signal.

2. Materials and methods

2.1. Studied combine harvesters

In this study, noise signals of John Deere 1055 and Sampo 3065 combine harvesters whose features are presented in Table 1 were measured and recorded in operational conditions. Examinations carried out in a completely randomised design with four replications. The studied variables included engine speeds (slow and fast), different gear ratios (natural, 1, 2, 3, and 4), op-

Table 1. Specifications of the combine harvesters.

	Specifications	Sampo	John Deere
Engine specifications	150	200	Power (hp)
	6	6	Number of cylinder
Other specifications	type of transmission	hydrostatic	synchromesh
	forward speed	3 stages	4 stages
	reverse speed	3 stages	1 stages
	steering	hydraulic	hydraulic
	working life	brand new	brand new

Table 2. Levels of measured parameters.

Parameters	Levels of parameters				
Engine speed	slow	fast			
Gear ratio	neutral gear	1st gear	2nd gear	3rd gear	4th gear
Type of operation	travelling	harvesting			
Microphone position	operator's ear with cabin		operator's ear without cabin		

eration status (travelling and harvesting), the location of the microphone in the combines with and without a cabin (Table 2). Since Sampo combine only has three forward gears, the variable of gear ratio has four levels for it.

During harvesting, the combine not only has transitional motion but also all parts of the harvest system including cutter bar, packer, straw rack, sieves, and blowers are moving. During the combine's free movement, it only has transitional motion and all other parts are inactive. Measuring the noise signals caused by the combines was carried out with and without cabin.

In order to measure the level of the combine noise in the location of the operator's ears, a microphone was placed at the distance of 100 mm from the operator's ear. The characteristics of the test location were based on the standards of International Organization for Standardization (ISO 5131 and ISO 7216). In so doing, an open area in Iran's Combine Manufacturing Factory and away from any sound reflector such as buildings and trees was selected. During the test, wind speed was measured using a digital anemometer, and it was recorded to be below 5 m/s in all tests. Since all tests were carried out during summer, the temperature was constantly over 5°C. Therefore, both wind speed and temperature were according to the conditions postulated in standard principles.

According to the standard based on which the test was carried out, the difference between the measured sound pressure level and the sound source during the work and background sound pressure should be at least 6 dB and preferably over 10 dB. In order to make the conducted measures reliable, the sound pressure level of background was measured only before the combines were put into operation. Since the background sound pressure was different from the combines' noises, there was no need to apply noise corrections into the background sound. A 30-meter rout was considered for the combines' movement. During the elapsed time for the combines to pass the mentioned distance, the signal of the released noise was measured. Equipment features used to measure the combines' sound pressure changes in time domain are presented in Table 3.

In each treatment combination, a 5-second noise signal was recorded. Afterwards, in the primary data analysis phase in time domain, 3-second pieces were selected out of the recorded 5-second pieces, those

Table 3. Specifications of the instruments.

Instruments	Sensitivity	Range	Model	Make
Microphone	50 mV/Pa	16–146 dB	MP201	BSWA
Pre-amplifier	–	19 Hz – 150 kHz	MAP231	BSWA
Data acquisition	–	35–118 dB	MC3022	BSWA
Calibrator	–	94 and 114 dB at 1000 Hz	CA111	BSWA
Digital anemometer	–	0.4–25 m/s	AM-4205A	Lutron

being almost uniform and with the least possible differences with other pieces (Fig. 1). After the tests and data collection, the collected data were analysed using MATLAB (2010 version) and SPSS 20.0.
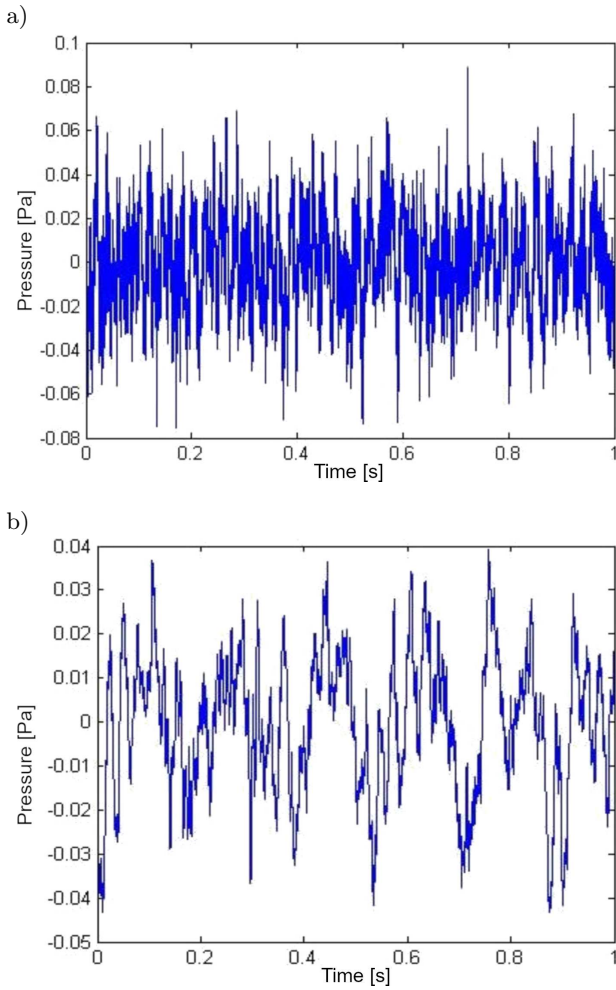
a)

b)

Fig. 1. Combine sound signals, position of the driver's ear a) without cabin and b) in the cabin.

In order to obtain the FD of the noise signals, the whole surface of the waveform by time intervals (window) with distances of 50, 100, and 200 ms was divided into smaller components. Between each of these intervals, a distance of 25 ms was also considered (Fig. 2). Afterwards, the FD was measured for each interval using the mentioned methods.

2.2. Fractal dimension

In physical systems, there is a maximum and minimum scale range in fractal objects for self-affine properties. In fact, when an event like a physiological signal occurs in nature, it repeats itself precisely on different scales (RAGHAVENDRA, NARAYANA DUTT, 2010). There are different methods to determine FD, and in this study some of them are discussed below.
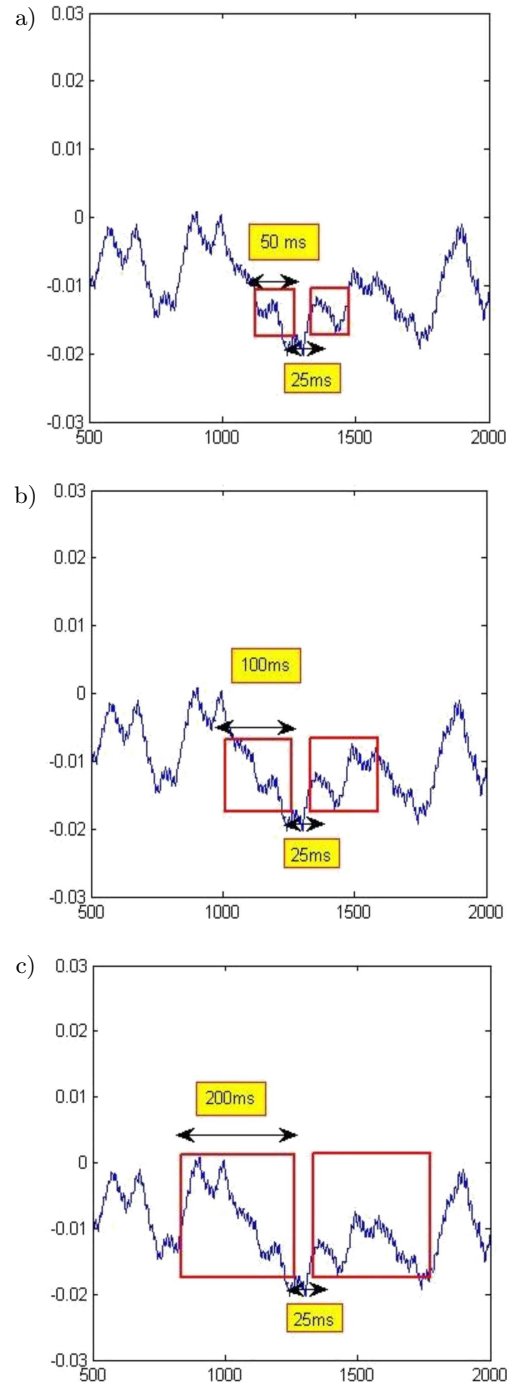
a)

b)

c)

Fig. 2. Distribution of window sizes on the audio signal: a) 50 ms, b) 100 ms, and c) 200 ms.

2.2.1. Katz's method

According to this method, the waveforms are like flat curves that are composed of ordered pairs (x, y), and the value of x increases as a single unit. To distinguish the fractal dimension of the waveforms in Katz's method, Eq. (1) is employed

$$\text{FD} = \frac{\log n}{\log n + \log\left(\frac{d}{L}\right)}, \tag{1}$$

where n is the number of the phases in waveform, d is the spatial development of waveform, and L is the total length of wavelength. Therefore, the waveform has a range of fractal dimensions from 1 for direct lines to 1.5 for further complex waves (KATZ, 1988).

2.2.2. Sevcik method

In 1998, Sevcik made some changes to Katz's method, including normalisation of x and y axes before calculation of fractal dimension.

$$x_i^* = \frac{x_i}{x_{\max}}, \qquad (2)$$

$$y_i^* = \frac{y_i - y_{\max}}{y_{\max} - y_{\min}}, \qquad (3)$$

where x_i and y_i determine the coordinate of the i-th point, and $x_{\max}$, $y_{\max}$, and $y_{\min}$ indicate the maximum and minimum values of each window, respectively. Therefore, in the case of the total length of a signal that includes N samples is L, the fractal dimension will be defined as follow:

$$FD = 1 + \frac{\ln(L) + \ln(2)}{\ln(2N')}, \qquad (4)$$

and $N' = N - 1$ (SEVCIK, 2006).

2.2.3. Higuchi's method

In this method, fractal dimension of waveforms is defined as follows. If $x(1)$, $x(2)$, ..., $x(N)$ is the time series under analysis, the new time series of x_m^k is made in the following way:

$$x_m^k = \left\{ x(m), x(m+k), x(m+2k), ..., \right.$$

$$\left. x\left(m + \left\lfloor \frac{N-m}{k} \right\rfloor k\right)\right\}, \quad m = 1, 2, ..., k, \quad (5)$$

where m is the value of the initial time, k is the separate time distance between the points (delay), and $\lfloor a \rfloor$ is the integer of a. For each curve or time series x_m^k was made and the mean length of $L_m(k)$ was defined as follows:

$$L_m(k) = \frac{\sum\limits_{i=1}^{\lfloor (N-m)/k \rfloor} |x(m+ik) - x(m+(i-1)k| \,(n-1)}{\left\lfloor \frac{N-m}{k} \right\rfloor k}, \qquad (6)$$

where N is the length of the whole data statements x and are the $(N-1)/\lfloor (N-m)/k \rfloor k$ normalisation factor. The mean length for all of the time series has an equal delay of k. This process is repeated for all ks in the range from 1 to $k_{\max}$. The total of mean lengths for each k is defined as follows:

$$L(K) = \sum_{m=1}^{k} L_m(k). \qquad (7)$$

The total of mean lengths for k scale and $L(k)$ is according to k^{-D}, and D is the fractal dimension according to Higuchi's method. In the curve of $\ln(L(k))$ opposite to $\ln(1/k)$, the slope of the minimum linear squares that has the best accordance with the graph is the estimation obtained from fractal dimension (HIGUCHI, 1988).

2.2.4. Multiresolution box counting (MRBC) method

In this method, it is supposed that the tested signal has the sample frequency of N and f_s of all sample points of the signal. Sampling of N and f_s is considered as two successive points of $S(i)$ and $S(i+1)$ in the first phase on the graph. The time distance between these two points is $\mathrm{d}t = x(i+1) - x(i) = \frac{1}{fs}$. The height between them is $\mathrm{d}t = x(i+1) - x(i) = \frac{1}{fs}$. The size of the boxes required to cover these points is $\mathrm{d}t$ and the number of the boxes to cover the points is $b(i) = \lceil |h| / \mathrm{d}t \rceil$. $\lceil a \rceil$ is the biggest figure near a. Now the value of $y(i+1)$ is updated as follows. If $h > 0$, then $y(i+1) = y(i) + |h| - \mathrm{d}t$ and if $h < 0$, then $y(i+1) = y(i) - |h| + \mathrm{d}t$. This process is repeated for all points on the curve so as to reach the final point. The total number of the boxes needed to completely cover the curve with accuracy of r is equal to $B(r) = \mathrm{sum}(b(i))$ & $i = 1, 2, ..., N-1$.

In the next phase, the curve is divided with coarse time resolution, by decimating the cure by a factor of two. In other words, the points on the time axis of the curve were considered alternatively, i.e. $r = 2/fs$. Now, the size of the required boxes to cover the curve completely is as $\mathrm{d}t = 2/fs$. By repeating the above phases for various time accuracies, the number of the boxes $B(r)$ is obtained to cover the curve in $r = \frac{1}{fs} \cdot \frac{2}{fs} ..... \frac{R}{fs}$, where, R/fs is the maximum amount of time accuracy in which the curve finally locates. Ultimately, the slope of the diagram $\log(B(r))$ against $\log(1/r)$ is an estimation of fractal dimension of time signal using MRBC method (RAGHAVENDRA, NARAYANA DUTT, 2010).

3. Results

Table 4 presents the results of variance analysis related to the fractal dimension at different levels of engine speed, the position of the microphone, gear ratio, box length, type of operation, and calculation method for the two studied combines. It should be noted that the interaction effects among the three variables were neglected. The results indicate that the effects of engine speed, type of operation, microphone position, gear ratio, box length, and the method of calculating the fractal dimension were significant at a level of 1%. All interaction effects of the variables on fractal dimension were significant.

Table 5 presents FD and sound pressure level (SPL) means of different levels of gear ratio vs type of operation for the Sampo and John Deere combines. The

Table 4. Analysis of variance of engine speed, position of the microphone, gear ratio, and method of calculating on the FD for the Sampo and John Deere combines.

Degree of freedom	Source of variable	Mean Squares of FD	
		Sampo	John Deere
Engine speed	1	29.210**	100.330**
Operation	1	71.160**	18.700**
Mic psition	1	681.110**	26.980**
Gear	3	5.087**	2.810**
Box length	2	11.240**	20.690**
Method	3	143.370**	113.340**
Engine speed * Gear	3	0.066**	0.380**
Engine speed * operation	1	2.660**	12.250**
Engine speed * mic position	1	339.360**	0.067**
Engine speed * box length	2	0.119**	0.304**
Engine speed * method	3	9.394**	38.330**
Gear * operation	3	0.783**	2.470**
Gear * mic position	3	0.835**	1.230**
Gear * box length	6	0.015**	0.019**
Gear * method	9	0.690**	0.390**
Operation * mic position	1	33.530**	0.135**
Operation * box length	2	0.289**	0.048**
Operation * method	3	6.177**	15.210**
Mic position * box length	2	0.060**	0.063**
Mic position * method	3	26.290**	36.130**
Box length * method	6	7.710**	8.750**

** Significant at level 1%.

Table 5. Fractal dimension (FD) and sound pressure level (SPL) means of different levels of gear ratio *vs* type of operation for the Sampo and John Deere combines.

	John Deere				Sampo			
	Travelling		Harvesting		Travelling		Harvesting	
	FD	SPL [dB]	FD	SPL [dB]	FD	SPL [dB]	FD	SPL [dB]
Neutral gear	1.50	96.40	1.54	104.20	1.35	93.80	1.43	98.40
1st gear	1.48	98.10	1.54	105.90	1.38	93.60	1.45	99.01
2nd gear	1.51	97.20	1.56	104.70	1.35	94.90	1.44	99.00
3rd gear	1.52	95.70	1.55	103.80	1.34	96.60	1.45	103.30
4th gear	1.57	103.20	1.56	110.40	–	–	–	–

results showed that the maximum means FD/SPL of noise signals in the travelling position in John Deere and Sampo combines were 1.57/103.2 and 1.38/93.6 for 4th and 1st gear, respectively, and minimum of these values for John Deere and Sampo combines in the travelling operation were 1.48/98.1 and 1.34/96.6 for 1st and 3th gear, respectively. While the maximum means FD/SPL of noise signals in the harvesting position in John Deere and Sampo combines were 1.56/110.4 and 1.45/103.3 for 4th and 3th gear, respectively, and minimum of these values for John Deere and Sampo combine in the harvesting position were 1.54/104.2 and 1.43/98.4 both for natural gear, respectively. As seen, both combines had a higher FD and SPL in the har-

vesting position. Therefore, complexity of combines' noise signal increased in the harvesting position according to the definition of the sound pressure level (Maleki, Lashgari, 2014). It can be stated that the wave disturbance rate is higher in the harvesting position than in the travelling one.

Figure 3 indicates that in Sampo combine, FD decreased with an increase in gear ratio for fast and slow engine speed. The maximum mean of FD was obtained in natural and 1st gear for fast and slow engine speed, respectively. However, in John Deere combine, the maximum mean of FD was obtained in the 4th gear for both fast and slow engine speed. In other words, as opposed to Sampo, FD increases with an increase in
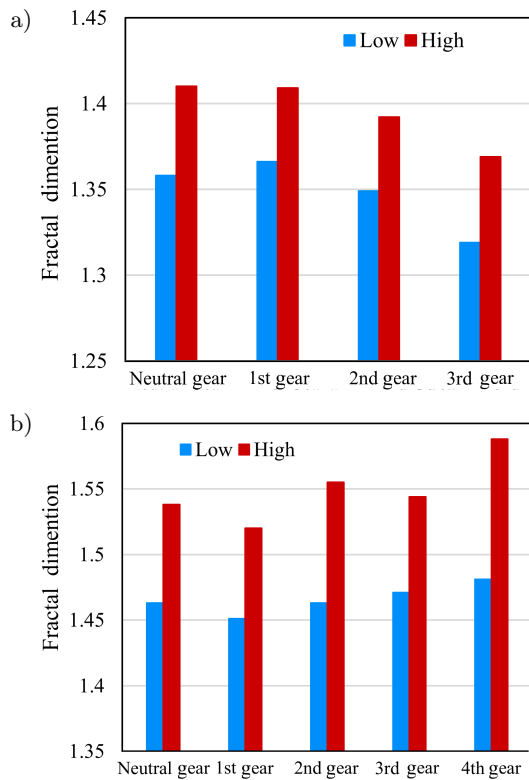
Fig. 3. Interaction effect of engine speed and gear ratio in: a) John Deere combine and b) Sampo combine.
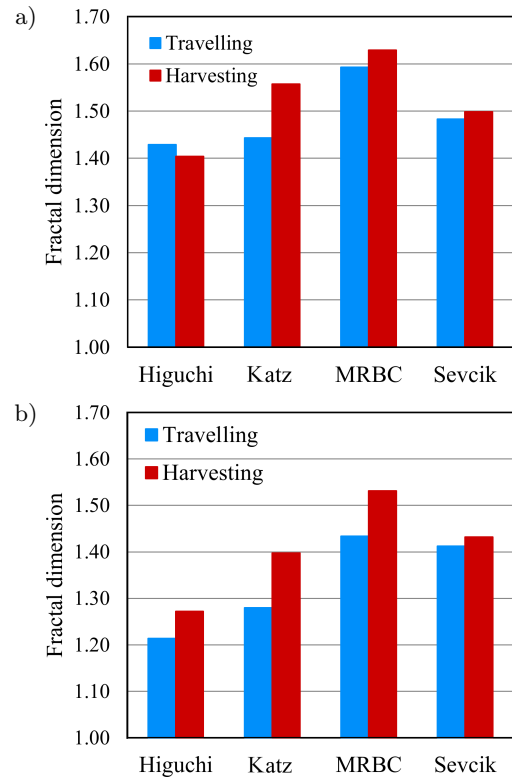

Fig. 4. Interaction effect of operating conditions and calculating fractal dimension methods in: a) John Deere combine and b) Sampo combine.

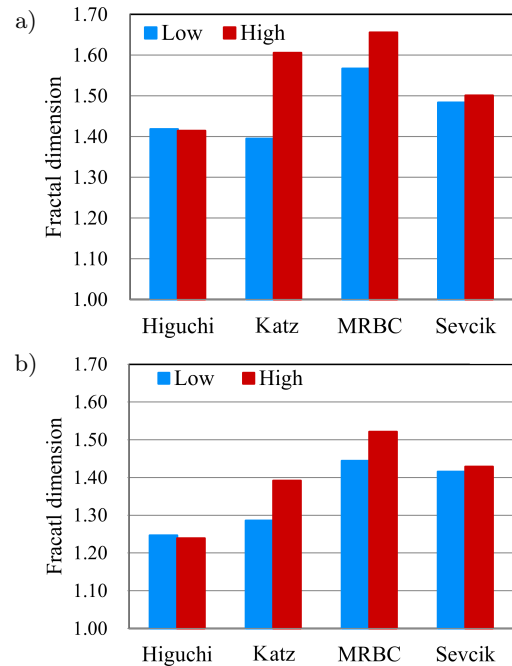
Fig. 5. Effect of the engine speed and calculating methods on fractal dimension in: a) John Deere combine and b) Sampo combine.

gear ratio in John Deere. This difference could be attributed to the fact that the gearbox of Sampo combine is hydrostatic, while John Deere has a synchromesh gearbox. In general, the Sampo combine has a smaller fractal dimension and low complexity in noise signals.

In addition, means of FD of noise signals in both combines were calculated during travelling and harvesting position by different methods (Fig. 4). As observed, the harvesting position is accompanied with a higher FD as compared to the travelling position. Only in John Deere combine and using Higuchi's method did harvesting position have a lower FD. Since the parts related to the harvester, picker, cleaner, and transmitter are in operation and movement of these parts led to an increase in the sound pressure level and complexity of noise signals due to the contact among metal parts, therefore, it is obvious to witness an increase in FD.

Figure 5 shows the effect of different levels of engine speed and the method of calculating FD in the two combines. As indicated, in Higuchi's method, no significant difference was observed in fractal dimension of the signal, with an increase in the engine speed. In general, the difference between the maximum and minimum amounts of FD in Higuchi's, Katz's, MRBC, and Sevcik's methods while increasing the engine speed in John Deere combine were 0.99, 1.15, 1.05, and 1.01 and in Sampo they were 0.993, 1.08, 1.05, and 1.00, respectively. In other words, the calculated FD was higher

for fast engine speeds in all methods for John Deere than Sampo. Compared to other methods, Higuchi's and MRBC led to the least and the most amounts of FD, respectively.

Table 6. Fractal dimension (FD) and sound pressure level (SPL) means of different levels of engine speed in/out of cabin for the Sampo and John Deere combines.

| | John Deere | | | | Sampo | | | |
| | In the cabin | | Out the cabin | | In the cabin | | Out the cabin | |
	FD	SPL [dB]	FD	SPL [dB]	FD	SPL [dB]	FD	SPL [dB]
Slow	1.49	93.1	1.44	96.8	1.23	92.3	1.46	97.1
Fast	1.57	101.4	1.53	105.2	1.29	97.8	1.51	104.1

Table 6 presents FD and SPL means of different levels of engine speed in/out of cabin for the Sampo and John Deere combines. As it can be seen, the maximum and minimum means FD/SPL of noise signals in John Deere combine were 1.57/101.4 and 1.44/96.8 for in and out of cabin, respectively. The maximum and minimum means FD/SPL of noise signals in Sampo combine were 1.51/104.1 and 1.23/92.3 for in and out of cabin, respectively. According to the definition of the sound pressure level, increase in the sound level can result in the waveform graph irregularity, and thus FD will increase with an increase in the engine speed (Dewangan *et al.*, 2005). It can be stated that the wave disturbance rate is higher for the fast engine speed.

Figure 6 indicates the mean values of fractal dimension for engine speeds in the presence and absence of a cabin. In both combines, fractal dimension increased with an increase on the engine speed. In Sampo combine, the fractal dimension at two engine speeds increased from 1.46 and 1.51 to 1.23 and 1.29 in and out of cabin, respectively. However, in John Deere these values changed from 1.57 for the fast engine speed and 1.49 for the slow engine speed to 1.53 and 1.44 in and out of cabin, respectively. In other words, cabin in John Deere enhanced the amount of fractal dimension and did not damp noise signals.

The mean amount of fractal dimension for the noise signals of Sampo combine in a window with the length of 50 ms was 1.35. At the same time, boxes of 100 and 200 ms received fractal dimensions of 1.37 and 1.40, respectively. In John Deere combine, the fractal dimension amounts of 1.47, 1.50, and 1.53 belonged to boxes with lengths of 50, 100, and 200 ms. In other words, with an increase of the window length and the number of the data available in each window, the fractal dimension increases (Gnitecki, Moussavi, 2005). As indicated in Fig. 7, in order to obtain the appro-
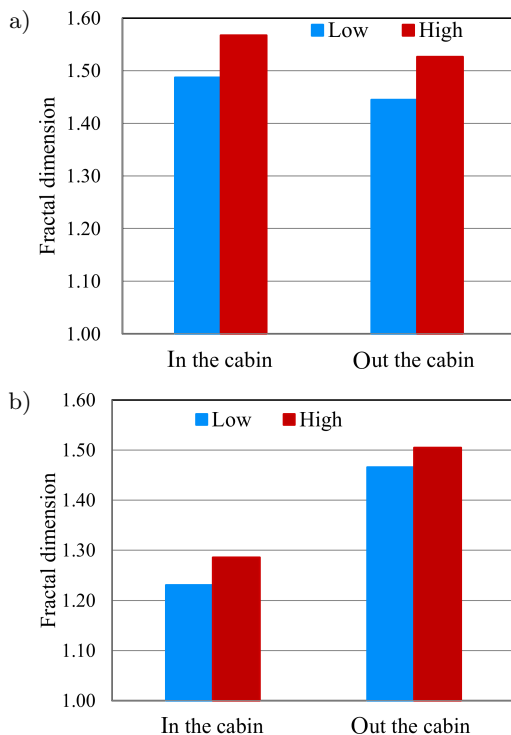

Fig. 6. Interaction effect of the engine speed and microphone positions at: a) John Deere Combine and b) Sampo combine.
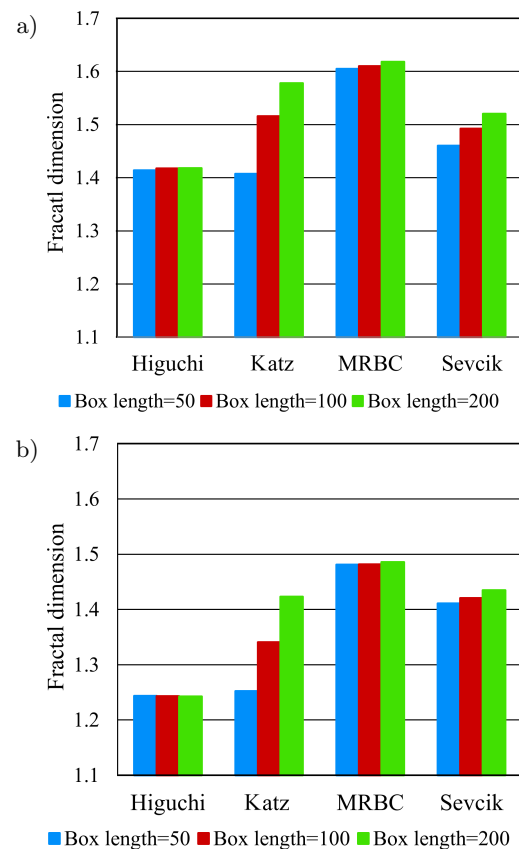

Fig. 7. Effect of changes in the window's length for different methods of calculating of fractal dimension at: a) John Deere combine and b) Sampo combine.

priate size of the window for fractal dimension, the extraction method is significant. Methods of Higuchi and MRBC indicated the least sensitivity to the change in the length of the time interval; therefore, these two methods are reliable.

4. Discussion and conclusion

Since noisy workplaces affect the efficiency of individuals' mind, concentration, accuracy, and reaction time, their final productivity and efficiency will drop. Therefore, it is necessary to provide combine operators' workplace with conditions that would minimize the noise effect as much as possible. Noise reduction in machinery is generally possible using two ways: active method by reducing the noise produced by noise producing sources such as engine, and inactive method, which is realised using the cabin and ergonomic design (BILSKI, 2013). Using the cabin on combine harvesters is one of the most effective methods to decrease the level of the operators' encounter with noise. The results of the study carried out by AYBEK *et al.* (2010) also indicated that using an appropriate cabin on tractors can reduce the sound level between 4 and 18 dBA. This reduction in SPL reduces the level of disturbance and confusion in the waveform in time domain; therefore, it is expected that in case of the cabin's presence the amount of FD/SPL in Sampo combine will drop, while in John Deere combine the opposite situation was observed. This can be attributed to the fact that the measured noise inside the cabin is composed of the structural and airborne noises. In John Deere, the cabin does not decrease the noise, it only prevents the encounter of the operator with dust and outside elements.

With an increase in the length of the sliding windows and the engine speed of the combines, the amount of the FD increased. In other words, the size of the suitable window depends on the extraction method of calculating the FD. In this study, Higuchi's method measured the minor changes in values of FD in all conditions and methods, with the minimum mean of 1.41 and 1.24 for John Deere and Sampo combines, respectively. The maximum amount of FD was measured using MRBC method, which was 1.6 and 1.48 for John Deere and Sampo combines, respectively.

The results also showed that the type of the gearbox used in the combines could have a tangible effect on the change trend in the FD while enhancing the gear ratio. Maximum means FD/SPL of noise signals in the harvesting position in John Deere and Sampo combines were 1.56/110.4 and 1.45/103.3 for 4th and 3th gear, respectively, which proves that complexity of combines' noise signal increased for higher gears and harvesting position.

References

1. AYBEK A., KAMER H.A., ARSLAN S. (2010), *Personal noise exposures of operators of agricultural tractors*, Applied Ergonomics, **41**, 274–281.

2. BACKES A.R., BRUNO O.M. (2010), *Shape classification using complex network and multi-scale fractal dimension*, Pattern Recognition Letters, **31**, 44–51.

3. BILSKI B. (2013), *Exposure to audible and infrasonic noise by modern agricultural tractors operators*, Applied Ergonomics, **44**, 2, 210–214.

4. BOHEZ E.L.J., SENEVIRATHNE T.R. (2001), *Speech recognition using fractals*, Pattern Recognition, **34**, 2227–2243.

5. BRUNO O.M., PLOTZE R.O., FALVO M., CASTRO M. (2008), *Fractal dimension applied to plant identification*, Information Sciences, **178**, 2722–2733.

6. DEWANGAN K., KUMAR G., TEWARI V. (2005), *Noise characteristics of tractors and health effect on farmers*, Applied Acoustics, **66**, 1049–1062.

7. EHLERS J.J., GRAYDON P.S. (2011), *Noise-induced hearing loss in agriculture: Creating partnerships to overcome barriers and educate the community on prevention*, Noise Health, **13**, 51, 142–146.

8. ESTELLER R., VACHTSEVANOS G., ECHAUZ J., LITT B. (2001), *A comparison of waveform fractal dimension algorithms*, IEEE Transactions on Circuits and Systems I: Fundamental Theory and Applications, **48**, 2, 177–183.

9. FLORINDO J.B., BRUNO O.M. (2011), *Closed contour fractal dimension estimation by the Fourier transform*, Chaos, Solitons and Fractals, **44**, 851–861.

10. GNITECKI J., MOUSSAVI Z. (2005), *The fractality of lung sounds: A comparison of three waveform fractal dimension algorithms*, Chaos, Solitons, and Fractals, **26**, 1065–1072.

11. GOMEZ C., MEDIAVILLA A., HORNERO R., ABASOLO D., FERNANDEZ A. (2009), *Use of the Higuchi's fractal dimension for the analysis of MEG recordings from Alzheimer's disease patients*, Medical Engineering and Physics, **31**, 306–313.

12. GRIFT T.E., NOVAIS J., BOHN M. (2011), *High-throughput phenotyping technology for maize roots*, Biosystems Engineering, **110**, 40–48.

13. HIGUCHI T. (1988), *Approach to an irregular time series on the basis of the fractal theory*, Physica D: Nonlinear Phenomena, **31**, 2, 277–283.

14. ISO 5131 (1996), *Acoustics: Tractors and machinery for agriculture and forestry measurement of noise at operator's position.*

15. ISO 7216 (1992), *Acoustics: Agricultural and forestry wheeled tractors and self-propelled machines, Measurement of noise emitted when in motion.*

16. Katz M.J. (1988), *Fractals and the analysis of waveforms*, Computers in Biology and Medicine, **18**, 3, 145–156.

17. Klonowski W., Olejarczyk E., Stepien R. (2005), *Sleep-EEG analysis using Higuchi's fractal dimension*, International Symposium on Nonlinear Theory and its Applications, 18–21 October, Bruges, Belgium.

18. Maleki A., Lashgari M. (2014), *Analysis of combine harvester sound pressure level in one-third octave band frequency*, Journal of Agricultural Machinery, **4**, 2, 154–165.

19. McBride D.I., Firth H.M., Herbison G.P. (2003), *Noise exposure and hearing loss in agriculture: A survey of farmers and farm workers in the Southland region of New Zealand*, Journal of Occupational and Environmental Medicine, **45**, 12, 1281–1288.

20. Raghavendra B.S., Narayana Dutt D. (2010), *Computing fractal dimension of signals using multi-resolution box-counting method*, World Academy of Science, Engineering and Technology, International Journal of Electrical, Computer, Energetic, Electronic, and Communication Engineering, **4**, 1, 183–198.

21. Rangayyan R.M., Oloumi F., Wu Y., Cai S. (2013), *Fractal analysis of knee-joint vibrio orthographic signals via power spectral analysis*, Biomedical Signal Processing and Control, **8**, 23–29.

22. Sabanal S., Nakagawa M. (1996), *The fractal properties of vocal sounds and their application in the speech recognition model*, Chaos, Solitons and Fractals, **7**, 11, 1825–1843.

23. Sevcik C. (2006), *On fractal dimension of waveforms*, Chaos, Solitons, and Fractals, **28**, 579–580.

24. Xie H., Zhou H.W. (2008), *Application of fractal theory to top-coal caving*, Chaos, Solitons and Fractals, **36**, 797–807.

25. Xie H.P., Liu J.F., Ju Y., Li J., Xie L.Z. (2011), *Fractal property of spatial distribution of acoustic emissions during the failure process of bedded rock salt*, International Journal of Rock Mechanics and Mining Science, **48**, 1344–1351.